

# The Effect of X-ray Irradiation on the Time Dependent Behaviour of Accretion Disks with Stochastic Perturbations.

Bari Maqbool<sup>1\*</sup>, Ranjeev Misra<sup>2</sup>, Naseer Iqbal<sup>1,2</sup> and Naveel Ahmad<sup>1</sup>

<sup>1</sup> *Department Of Physics, University of Kashmir, Srinagar-190006, India*

<sup>2</sup> *Inter-University Center for Astronomy and Astrophysics, Post Bag 4, Ganeshkhind, Pune-411007, India*

## ABSTRACT

The UV emission from X-ray binaries, is more likely to be produced by reprocessing of X-rays by the outer regions of an accretion disk. The structure of the outer disk may be altered due to the presence of X-ray irradiation and we discuss the physical regimes where this may occur and point out certain X-ray binaries where this effect may be important. The long term X-ray variability of these sources is believed to be due to stochastic fluctuations in the outer disk, which propagate inwards giving rise to accretion rate variation in the X-ray producing inner regions. The X-ray variability will induce structural variations in the outer disk which in turn may affect the inner accretion rate. To understand the qualitative behaviour of the disk in such a scenario, we adopt simplistic assumptions that the disk is fully ionised and is not warped. We develop and use a time dependent global hydrodynamical code to study the effect of a sinusoidal accretion rate perturbation introduced at a specific radius. The response of the disk, especially the inner accretion rate, to such perturbations at different radii and with different time periods is shown. While we didn't find any oscillatory or limit cycle behaviour, our results show that irradiation enhances the X-ray variability at time-scales corresponding to the viscous time-scales of the irradiated disk.

**Key words:** accretion: accretion discs - X-rays: binaries.

## 1 INTRODUCTION

Accretion disks are formed when matter from a companion star accretes on to a compact object which is usually a black hole or a neutron star. The structure of such disks can be described in the “ $\alpha$ -disk” prescription (Shakura & Sunyaev 1973) which is often referred to as the standard accretion disk model. Most of the energy is released in the inner regions of the disk and is radiated at X-ray energies and hence these systems are observed as X-ray binaries. The flux generated and the temperature of the disk decreases with radius and hence the outer regions of the disk emit in UV or in the optical. However, there are couple of ways by which the outer region of the disk effects the X-ray emission from the inner parts. If the outer region is non-ionised the disk becomes unstable. This hydrogen ionised thermal instability leads to a long term limit cycle like variability in the accretion rate (Cannizzo & Wheeler 1984). This is believed to be the origin of X-ray novae where an X-ray binary rises from quiescence on a time-scale of days and subsequently its lu-

minosity decays in months time-scale. X-ray novae typically recur in time-scales of decades. For persistent X-ray binaries, the outer disk is perhaps always ionised and hence such systematic long term variation is not seen. However, even for such persistent sources the X-ray emission displays stochastic variability in a wide range of time-scales ranging from milli-seconds to months. While the short term variability should arise from the inner regions, it is the outer regions which is thought to be responsible for the long term variation. A popular model for the long term variability is the stochastic fluctuation model (Lyubarskii 1997) where fluctuations in different radii of the disk, induce accretion rate variations in the viscous time-scale of that radius. These accretion rate variations then propagate inwards and cause the observed long term X-ray variability. Thus, the outer region of an X-ray disk effects the X-ray emission from the inner parts by regulating the accretion rate inflow into the inner region.

On the other hand, as noted and described by Cunningham (1976), the X-ray irradiation by the inner regions can affect the structure of the outer one. There have been several works to understand the struc-

\* E-mail: barispn1@gmail.com

ture and the resultant spectra of the outer regions in the presence of X-ray irradiation (e.g. Hayakawa 1981; Hoshi and Inoue 1988; Tuchman et al. 1990; Ko & Kallman 1991; Dubus et al. 1999; Hubeny and Wickramasinghe 2004; Wickramasinghe and Hubeny 2005; Ritter 2008; Mescheryakov et al. 2011). The reprocessed emission will be emitted in UV/optical and the spectra of such disks has been calculated and compared to observations (Vrtilek et al. 1990; Hayakawa 1981; Ritter 2008). The detailed vertical structure of such disks which depends on the radiative and heat transfer processes have been studied to better understand their spectral properties (Hubeny and Wickramasinghe 2004; Wickramasinghe and Hubeny 2005; Tuchman et al. 1990; Soon-Wook et al. 1999; Mescheryakov et al. 2011). The global structure of such irradiated disks is also expected to be complex with several studies showing that the disk may be warped or inflated (Hayakawa 1981; Dubus et al. 1999). The effect on the stability of the disk, especially on the thermal hydrogen ionised instability during an X-ray novae outburst has been studied (Ko & Kallman 1991; Ritter 2008) and found to be important.

Thus, this is an interesting situation where, while the accretion rate in the inner regions (and hence the X-ray flux) can be modulated by the outer disk, the outer disk itself can be strongly affected by the variations in the X-ray flux. In such systems involving feedback, there are possibilities of characteristic behaviour such as limit cycle oscillations, resonance or enhanced variability. We study here these effects by computing the response of such an X-ray irradiated disk to perturbations, using a global time dependent hydrodynamic code. For simplicity and to understand the basic phenomenon, we restrict the analysis to fully ionised disks without warps.

In the next section, we describe the steady state X-ray irradiated disks and quantify the regions of such disk where irradiation changes the disk structure. Using the known orbital properties of some X-ray binaries, we estimate whether their outer disks are expected to be influenced by X-ray irradiation. We then proceed in §3 to describe the time dependent accretion disk equations and present the results of the computation in §4. In §5 we summarise and discuss the work.

## 2 STEADY STATE STRUCTURE OF X-RAY IRRADIATED ACCRETION DISKS

In the  $\alpha$ -prescription used in the standard accretion disk model (Shakura & Sunyaev 1973), the angular momentum transfer equation is given by

$$\frac{\partial}{\partial r} [4\pi\alpha Pr^2 h] = \dot{M} \frac{\partial}{\partial r} [(GM/r)^{1/2}] \quad (1)$$

where  $M$  is the black hole mass,  $\dot{M}$  is the accretion rate,  $r$  is the radius and  $\alpha$  is the viscous parameter. For steady state, when  $\dot{M}$  is a constant and independent of radius, the equation can be integrated to give,

$$(\alpha P)(2\pi r \times 2h)(r) = \dot{M}(GM/r)^{1/2} \quad (2)$$

In order to study the structure of the outer disk, we neglect the inner boundary condition and consider the pressure,  $P = 2\rho kT/m_p$  to be the ionised pressure of a gas at

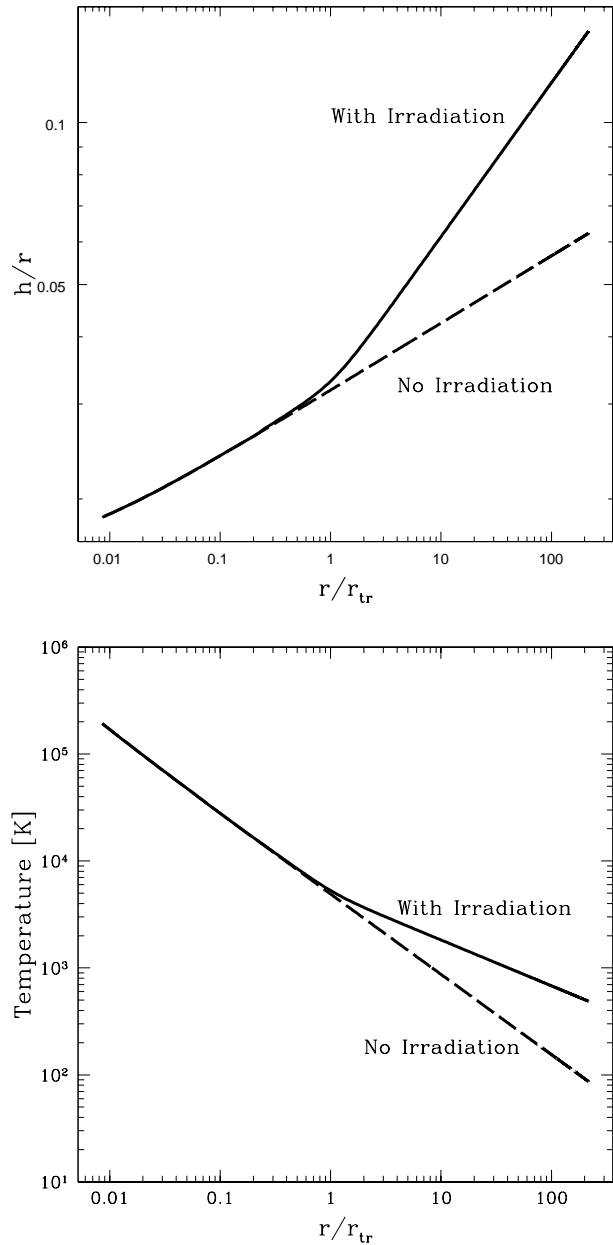


**Figure 1.** The normalised scale height ( $h/r$ ) of the accretion disk versus radii normalised to the transition radius obtained using fixed values of  $\dot{M} = 10^{17} \text{ gs}^{-1}$ ,  $\alpha = 0.1$  and  $\eta = 0.05$ . The solid line corresponds to the case when X-ray irradiation is considered while the dotted line is when the effect is not considered. For radii greater than the transition radius the disk has a larger height and temperature for the case when irradiation is considered as compared to when it is not. Note that the transition to the irradiation dominated region is fairly sharp.

temperature  $T$  and density  $\rho$ . The half-thickness of the disk,  $h$  can be estimated using hydrostatic equilibrium in the vertical direction to be

$$\frac{P}{\rho} \sim \frac{2kT}{m_p} \sim \left( \frac{GM}{r^3} \right) h^2 \quad (3)$$

The gravitational energy generated per unit area of the

disk is given by

$$F_o(r) = \frac{3\dot{M}}{8\pi r^2} \frac{GM}{r} \quad (4)$$

and in the standard disk, this is balanced by the radiative energy transfer in the vertical direction i.e.  $\sim \sigma T^4/\tau$ , where  $\tau$  is the optical depth given by the surface density  $\Sigma = \rho h$  times the opacity  $\kappa$ . In the presence of X-ray irradiation, there is an additional heating term  $F_{ir}$ . In the special case, when  $F_{ir} \gg F_o$ , and if one considers the disk to be vertically iso-thermal, the radiative flux should be  $\sigma T^4 \sim F_{ir}$  (Vrtilek et al. 1990). Here we follow Dubus et al. (1999) to write a general equation of the form

$$\sigma T^4 = F_o(r)[\Sigma(\bar{\kappa}_{ff} + \bar{\kappa}_{es})] + F_{ir}(r, h) \quad (5)$$

where we have considered both the opacity due to electron scattering  $\bar{\kappa}_{es}$  and due to free-free interaction  $\bar{\kappa}_{ff}$ . Opacity due to free-free interaction is given by Kramer's opacity law which is written as

$$\bar{\kappa}_{ff} = 0.64 \times 10^{23} \rho T^{-7/2} \text{ cm}^2 \text{ g}^{-1} \quad (6)$$

The heating due to X-ray irradiation is given by (Vrtilek et al. 1990)

$$F_{ir}(r, h) = \frac{f_2 L_x}{4\pi r} \frac{\partial h/r}{\partial r} \quad (7)$$

where  $f_2$  is the absorbed fraction of the radiation impinging on the surface and  $L_x$  is the X-ray luminosity which can be written as  $L_x = \eta \dot{M}_{in} c^2$ , where  $\eta$  is the radiative efficiency of the accretion and  $\dot{M}_{in}$  is the accretion rate in the inner region. For steady state,  $\dot{M}_{in}$  is the same constant accretion rate at every radii, but we denote it by a different symbol here for latter convenience.

The above equations can now be re-written to provide a differential equation after transforming  $r = x r_g$  and  $h = y r_g$  ( $r_g = GM/c^2$ ) to,

$$\frac{\partial y}{\partial x} = \frac{y}{x} + A_p x^{-10} y^8 - B_p x^{25/2} y^{-12} - C_p x^{1/2} y^{-2} \quad (8)$$

Where

$$A_p = \frac{4\pi\sigma r_g^2 c^6}{f_2 \eta \dot{M}_{in}} \left(\frac{m_p}{2k}\right)^4 \quad (9)$$

$$B_p = 6 \times 10^{21} \left(\frac{\dot{M}^3}{\dot{M}_{in} r_g^3 c^9}\right) \left(\frac{1}{\pi^2 \alpha^2 f_2 \eta}\right) \left(\frac{2k}{m_p}\right)^{7/2} \quad (10)$$

$$C_p = 0.375 \left(\frac{\dot{M}^2}{\dot{M}_{in} r_g c}\right) \left(\frac{\bar{\kappa}_{es}}{\alpha \pi f_2 \eta}\right) \quad (11)$$

This differential equation can be solved to obtain the height as a function of radius and subsequently one can obtain the temperature  $T$  and the surface density  $\Sigma$ . When irradiation dominates the gravitational energy release ( $F_{ir} \gg F_o$ ) then the last two terms can be neglected and the solution is  $y \propto x^{9/7}$  corresponding to the solution reported by Vrtilek et al. (1990). In the opposite regime when,  $F_{ir} \ll F_o$ , then there are two cases. If the opacity is dominated by scattering,  $\kappa_{es} \gg \kappa_{ff}$ , then the equation reduces to  $A_p x^{-10} y^8 = C_p x^{1/2} y^{-2}$  and when  $\kappa_{es} \ll \kappa_{ff}$ , it becomes  $A_p x^{-10} y^8 = B_p x^{25/2} y^{-12}$ . Solving the differential equation for  $\dot{M} = 10^{17}$  g/s,  $\alpha = 0.1$ , and  $\eta = 0.05$ , one obtains the scale height and the mid-plane temperature (Fig.

1). The outer radii where X-ray irradiation dominates has a higher temperature and scale height compared to what it would have been if there was not X-ray irradiation. The transition from viscous dominated to X-ray irradiated is rather sharp and the radius,  $r_{tr}$  where this occurs can be estimated from equating  $F_o(r_{tr})\Sigma\bar{\kappa}_{ff} \sim F_{ir}(r_{tr})$  which gives

$$r_{tr} \sim 2 \times 10^{11} \text{ cm} \left(\frac{\dot{M}}{10^{17} \text{ g/s}}\right)^{2/45} \left(\frac{M}{1.4 M_\odot}\right)^{11/9} \left(\frac{\alpha}{0.1}\right)^{-28/45} \quad (12)$$

where we have assumed (as is typically the case) that  $\bar{\kappa}_{ff} \gg \bar{\kappa}_{es}$ . Note that the transition radius is insensitive to the accretion rate ( $\propto \dot{M}^{2/45}$ ). The temperature of the disk at the transition region is given by

$$T(r_{tr}) \sim 4.9 \times 10^3 \text{ K} \left(\frac{\dot{M}}{10^{17} \text{ g/s}}\right)^{2/7} \left(\frac{M}{1.4 M_\odot}\right)^{-3/7} \quad (13)$$

Since we will be interested in the temporal behaviour of these disks, the viscous time-scale i.e. the radius divided by the local radial speed at the transition radius,

$$(T_{visc})_{tr} = 4 \times 10^7 \text{ secs} \times \left(\frac{\dot{M}}{10^{17} \text{ g/s}}\right)^{-11/45} \left(\frac{\alpha}{0.1}\right)^{71/45} \left(\frac{M}{1.4 M_\odot}\right)^{16/9} \quad (14)$$

sets a time-scale for any variability.

## 2.1 X-ray binaries with irradiated disks

An X-ray binary will have an X-ray irradiation dominated outer disk provided the transition radius (Eqn 12) is smaller than the extent of the disk. In a binary, as the matter flowing from the secondary to the primary possesses angular momentum, it will settle to a radius called the circularization radius which is given by (Frank, King, & Raine 2002)

$$R_{circ} = 4(1+q)^{4/3} [0.500 - 0.227 \log_{10} q]^4 P_d^{2/3} R_\odot \quad (15)$$

where  $q$  is the ratio of masses of the companion star and the compact object and  $P_d$  is the orbital period in days. Due to viscosity, angular momentum is transported outwards causing the disk to be larger than the circularization radius until it is disrupted by the tidal forces of the companion star. Typically, the Tidal radius  $R_T$  is related to the Circularization radius as  $R_T \sim 2R_{circ}$  (Shahbaz, Charles, & King 1998). Thus only systems with the transition radius  $r_{tr} < R_T$ , will have an outer disk whose structure is affected by X-ray irradiation.

We selected ten X-ray binaries from Low Mass X-Ray Binary Catalog, 4<sup>th</sup> edition (2007) and Zhang et al. (2011) for which the orbital period and the masses of the primary and companion are well constrained and list them in Table 1. There are three black hole candidates (BHC) and seven neutron star (NS) systems in the sample. We computed the circularization and tidal radii and compared it with the transition one. We have computed the transition radius for  $\alpha = 0.1$ , and accretion rates  $10^{17}$  g/s and  $10^{18}$  g/s for Neutron stars and black holes respectively. We find that for four of these sources (listed in the above panel of the table) the transition radius

**Table 1.** Comparison between the Circularization, Tidal and Transition Radii for some Low Mass X Ray Binaries.

Name	Type	$P_{orb}$ (d)	$M_1$ $M_\odot$	$M_2$ $M_\odot$	$R_c$ ( $10^{11} cm$ )	$R_T$ ( $10^{11} cm$ )	$r_{tr}$ ( $10^{11} cm$ )	$T$ (K)
4U 1811-17*	NS	24.0667	1.4	5	3.5	7.0	2.2	4900
3A1516-569*	NS	16.60	1.4	4	2.7	5.4	2.2	4900
CygX-2**	NS	9.84	1.780	0.63	2.5	5.0	2.9	4400
V395 CAR**	NS	9.02	1.44	0.35	2.7	5.4	2.3	4800
GS2023 + 338*	BHC	6.4750	12	0.6	4.1	8.2	33.7	3800
GRO J1655-40**	BHC	12.73	7	2.3	1.07	2.14	15.7	4700
XTE J2123-058**	NS	0.25	1.415	0.53	.22	0.44	2.2	4900
2A 1822-371**	NS	0.23	0.97	0.33	0.21	0.42	1.4	5700
GRS 1915 +105*	BHC	33.500	14	0.81	11.7	23.4	40.6	3500
2A 1822-371**	NS	1.7	1.5	2.3	0.6	1.2	2.4	4700

$M_1$  is the mass of the central compact object,  $M_2$  is the mass of the companion star,  $R_c$  is the Circularization radius,  $R_T$  is the Tidal radius and  $r_{tr}$  is the transition radius of the accretion disk. The temperature  $T$  is the temperature of the accretion disk at the transition radius. NS - Neutron Star. BHC - Black Hole Candidate.

\*(Zhang et al. 2011, and references therein), \*\* (Low Mass X-Ray Binary Catalog, 4<sup>th</sup> edition 2007).

is smaller than the tidal one, indicative that these systems may have an outer disk whose structure is affected by X-ray irradiation. We also computed the temperature at the transition radius. Typically the temperature is not high enough to justify that the disk is completely ionised, which has been discussed in the last section.

### 3 TIME-DEPENDENT ACCRETION DISK WITH X-RAY IRRADIATION

The surface density  $\Sigma$  will change with time if the accretion rate varies with radius and its behaviour is governed by the conservation of mass equation

$$\frac{\partial \Sigma}{\partial t} = \frac{1}{2\pi r^2} \frac{1}{x} \frac{\partial \dot{M}}{\partial x} \quad (16)$$

The angular momentum transfer equation (1) provides the accretion rate as a function of  $\Sigma$  and its derivative

$$\dot{M} = H \left[ -\Sigma x^{-3/2} y^2 + 2\Sigma \frac{\partial y}{\partial x} x^{-1/2} y + \frac{\partial \Sigma}{\partial x} x^{-1/2} y^2 \right] \quad (17)$$

where  $H = 4\pi\alpha(GMr_g)^{1/2}$ . Combined with Equation (16), this provided a second order partial differential equation in  $\Sigma$ , a diffusive type equation describing the temporal behaviour of the disk. The normalised scale height  $y = h/r_g$  is obtained from Equation 8, written in terms of  $\Sigma$ , i.e.

$$\frac{\partial y}{\partial x} = \frac{y}{x} + A'_p x^{-10} y^8 - B'_p \Sigma^3 x^8 y^{-6} - C'_p \Sigma^2 x^{-5/2} y^2 \quad (18)$$

Where

$$A'_p = \frac{4\pi\sigma r_g^2 c^6}{f_2 \eta \dot{M}_{in}} \left( \frac{m_p}{2k} \right)^4 \quad (19)$$

$$B'_p = 6.4 \times 10^{22} \left( \frac{6\pi\alpha}{f_2 \eta c^6 \dot{M}_{in}} \right) \left( \frac{2k}{m_p} \right)^{7/2} \quad (20)$$

$$C'_p = 6 \left( \frac{c r_g}{\dot{M}_{in}} \right) \left( \frac{\bar{\kappa}_{es} \pi \alpha}{f_2 \eta} \right) \quad (21)$$

In these equations, the local accretion rate  $\dot{M}(x, t)$  is different from the accretion rate at the inner radius  $x_{in}$ , denoted by  $\dot{M}_{in}(t) = \dot{M}(x_{in}, t)$ .

We solve the above set of differential equations using standard techniques and by imposing the courant condition  $\frac{2D\Delta t}{(\Delta x)^2} \leq 0.5$  for stability, where  $\Delta t$  is the variable time step,  $\Delta x$  is the bin size in the radius and  $D$  is the approximate diffusion coefficient of the time varying equation. We tested the code by evolving for several times the viscous time-scale of the outer radius and found the structure of the disk to be stable after a short transient phase. Next, we increase the accretion rate at the outer radius to twice its initial value and as expected after evolving for a time longer than the viscous time, the disk settled into a structure identical to the steady state for the enhanced accretion rate. The only issue, was that at small radii, when the disk is dominated by viscous heating (i.e. X-ray irradiation is not important), then the last three terms in Eqn 18 are large, making the derivative  $\frac{\partial y}{\partial x}$ , susceptible to numerical errors. In such cases, we use instead of Eqn 18, the expression for the height of the disk when X-ray irradiation is not important i.e.

$$A'_p x^{-10} y^8 - B'_p \Sigma^3 x^8 y^{-6} - C'_p \Sigma^2 x^{-5/2} y^2 = 0 \quad (22)$$

We do this change over when the scale heights computed by Eqn (18) and Eqn (22) differ by less than 5%. This scheme allows us to obtain in general, well behaved solutions both in time and in radius.

### 4 TIME-DEPENDENT SOLUTIONS

We solve the time-dependent equations for  $M = 1.4M_\odot$ , a steady state accretion rate of  $\dot{M}_s = 1e17$  g/s,  $\alpha = 0.1$  and the efficiency factor  $\eta = 0.05$ , as we are interested in understanding the temporal response of the disk to stochastic perturbations initiated at different radii and for different time periods. Thus at a radius which we call the perturbation radius  $x_p$ , we force the accretion rate to oscillate such

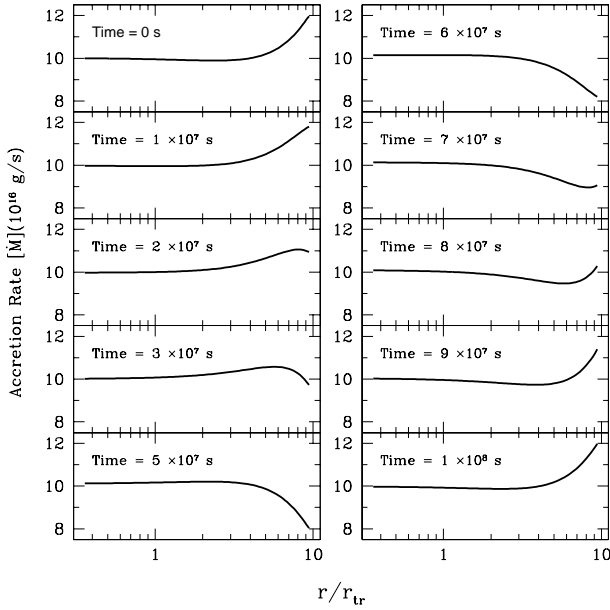


**Figure 2.** Snapshots of accretion rate versus radii at different times. The perturbation has been introduced at  $10r_{tr}$  and has a time period of  $1 \times 10^8 \text{ s} = 2.6 \times (T_{vis})_{tr}$

that  $\dot{M} = \dot{M}_s(1 + \Delta\dot{M} \sin(2\pi t/T_p))$ , where  $T_p$  is the time period of the oscillation and  $\Delta\dot{M}$  is the normalised amplitude there taken to be a few percent for the simulations.

If the time period  $T_p$  is significantly smaller than the viscous time-scale at a radius, the perturbation is expected to decrease rapidly as it moves inwards. On the other hand, if  $T_p$  is much larger than the viscous one, the perturbation will remain unchanged at smaller radii. Thus, the region of interest is the behaviour of the perturbation at radii where the viscous time-scales is of the similar order as the time period of the oscillations. In this work, to save numerical time, we introduce the perturbation at a radius where the viscous time-scale is 3 times the perturbation time period and follow its evolution to a radius where the viscous time-scale is roughly a tenth of the time period. Moreover, we expect interesting physical behaviour to occur at the transition radius and hence we restrict the analysis to perturbations with time periods close to the viscous time-scale at that radius which is  $\sim 4 \times 10^7 \text{ secs}$  (Eqn 14).

To a steady state disk we introduce a perturbation at the prescribed radius and wait for two times the viscous time-scale to allow for any transient behaviour to die down. We then continue the simulation for at least ten times the time period by which time the system has settled down to unchanging sinusoidal behaviour. We analyse the results only for the last 8 oscillations. A typical response of the system is shown in Figure 2 where time snap shots are shown of the accretion rate versus radius for one complete oscillation. The time period is  $10^8 \text{ sec} = 2.6 \times (T_{vis})_{tr}$  and is introduced at a radius which is roughly ten times the transition radius. It is clear from the Figure, that the perturbation damps out as it moves inwards and amplitude of the oscillation is rather small in the inner regions.

To quantify the behaviour we compute the r.m.s =

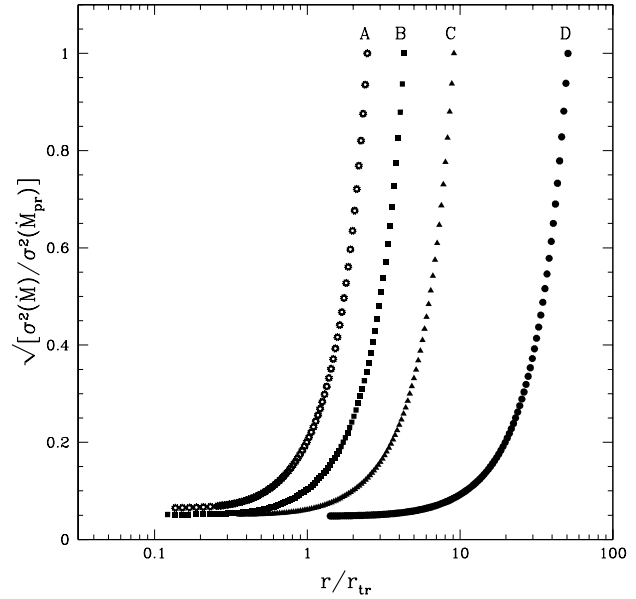


**Figure 3.** The root mean square (i.e. the square root of the variance  $\sqrt{\sigma^2}$ ) of the accretion rate perturbation as a function of radius. The r.m.s has been normalised to that introduced at the perturbation. The curves are plotted for four different time-periods. For the curves marked A, B, C and D, the time-periods are 0.8, 1.3, 2.6 and 13.0 times the viscous time-period at the Transition radius respectively. The amplitude of the perturbation decreases and then saturates with radius.

$\sqrt{\sigma^2(\dot{M})}$  at different radii. In Figure 3, we plot the r.m.s normalised to the r.m.s at the perturbation radius for different time periods. The behaviour of these curves are expected since for large radii, where the local viscous time-scale is longer than the time period of the perturbation, the r.m.s decreases sharply but becomes a constant at radii where the viscous time-scale is shorter. As mentioned before, we introduce the perturbation at a radius where the local viscous time scale is 3 times the time period. If the perturbation radius is chosen to be a larger one, we obtain the same behaviour as shown in the Figure 3, i.e. the curve starts at a larger radii but has the same shape for the range of radii.

Another perhaps more illustrative way to show the results is to note the ratio of the r.m.s of the accretion rate variation in the inner region to that at the radius of the perturbation i.e.  $\sqrt{\sigma^2(\dot{M}_{in})/\sigma^2(\dot{M}_{pr})}$  as a function of time period. This essentially tells us how the inner accretion rate (i.e. the X-ray emission) responds to a perturbation at a given outer radius. The ratio is plotted for different perturbation radii in Figure 4. The ratio is nearly unity when the time period is longer than the viscous time-scale and is significantly less than one, when the time period is smaller. To understand the effect of the X-ray irradiation, we also perform a mock simulation where the X-ray luminosity is artificially kept at the steady state value. The results of such simulations without X-ray feedback are plotted as dotted lines in Figure 4. When the perturbation is introduced at a radii less than the transition one (curve marked A) there is as expected no difference between the cases with and without feedback. However, when the perturbation is introduced



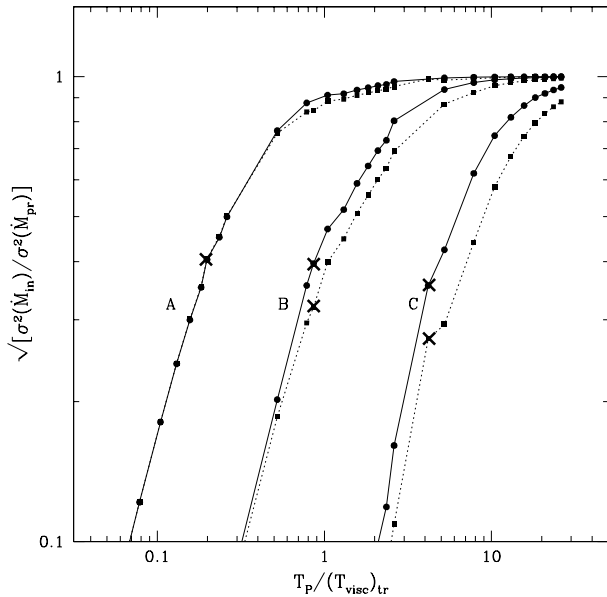


**Figure 4.** The root mean square variation of the inner accretion rate as a function of time period. For the curves marked A, B and C, the perturbation radii are 0.3, 1 and 5 times the transition radius respectively. The dotted lines are for the case when the X-ray luminosity is artificially kept constant at the steady state value i.e. when there is no feedback. The crosses on different curves correspond to the viscous time-scale at the corresponding perturbation radius.  $\sigma^2(\dot{M}_{in})$  is taken to be the variation at a radius where the viscous time-scale is roughly a tenth of the time period of the perturbation. When the perturbation is at a radius larger than the transition one, the induced inner accretion rate variation is greater than the case without feedback. This indicates that X-ray irradiation enhances the variability at time-scales larger than  $(T_{visc})_{tr}$ .

at radii larger than the transition one, the induced variation in  $\sigma^2(\dot{M}_{in})$  is larger for the case with feedback. This suggests that the effect of X-ray irradiation is to enhance the variability at time-scales larger than the viscous time-scale of the transition radius.

## 5 DISCUSSION

Our study of a time-dependent X-ray irradiated disk shows that the response of the inner accretion rate is different for a perturbation introduced in the X-ray irradiation dominated part of the disk compared to one at radii less than the transition one. Since the viscous time-scale at the transition radius is  $\sim 4 \times 10^7$  secs, this effect will be observable only by decades long monitoring of these sources. Using the All Sky Monitor (ASM) data of the RXTE satellite, Gilfanov & Arefiev (2005) have reported breaks in the power spectra of several X-ray binaries indicating that the power at frequencies below the break frequency is less than expected. This is in contrast to the results obtained in this work, which suggests that the variability at low frequency should be enhanced. More seriously, as noted by Gilfanov & Arefiev (2005), the break frequencies occur in the range  $10^{-5}$  -  $10^{-7}$  Hz which is much shorter than the viscous time-scale of the

outermost radius and the viscous time-scale of the transition radius. This indicates that the breaks reported by Gilfanov & Arefiev (2005) maybe a different phenomenon unrelated to the effects of X-ray irradiation studies here. However given that the ASM data is not continuous and maybe affected by systematic effects, it is difficult to make a comparison. Moreover, the results of this work are based on simplistic assumptions which may need to be lifted before a meaningful comparison with observations is possible.

We have assumed that the disk is fully ionised but the temperature estimated at the transition radius ( $T < 10^4$  K) indicates that the disk would be partially ionised. The most dominant effect would be that a partially ionized disk will have additional opacity due to absorption. The structure of the disk when X-ray irradiation dominates does not depend on the opacity and hence will not be affected. However, the transition radius may change leading to a different viscous time-scale where the effect of X-ray irradiation maybe observed. Thus while a time-dependent formalism that computes the ionisation state of the disk at each radii maybe challenging, it maybe required to predict the quantitative behaviour of the disk. Perhaps a more important effect which may change the qualitative nature of the result obtained here, is if the irradiated part of the disk is warped, especially if the warping follows any temporal X-ray modulation. A more sophisticated comprehensive treatment is required to understand the effects of these aspects.

An important future study would be to predict the time varying broadband spectrum from such X-ray irradiated disks. This would require estimating the effective temperature at each radius. While the structure of the disk is affected by the X-ray irradiation only beyond the transition radius, the effective temperature will depend on the time-dependent X-ray emission at much smaller radii. The UV/optical emission would have contribution from a span of radii where the effective temperature will have complex temporal behaviour. The study can predict the relative r.m.s variation as well as time-lags between the X-ray and different UV/optical bands. For some X-ray binaries there is evidence that the short time-scale correlation between the X-ray and optical band is complex i.e. although X-ray reprocessing could be a factor, the optical variability could also be due to other contributions such as a jet emission (e.g. Motch, Ilovaisky, & Chevalier 1982; Kanbach et al. 2001; Drappeau et al. 2014). This complex short as well as long term behaviour can be tested using data from the forthcoming X-ray satellite ASTROSAT (Agrawal 2006) which can simultaneously and sensitively measure the optical/UV and X-ray emission from such sources. Thus, the present work lays the foundation for future studies which will enhance our understanding of the outer accretion disks of X-ray binaries.

## 6 ACKNOWLEDGEMENTS

The authors are grateful to ISRO-RESPOND Program for providing the financial assistance under grant No. ISRO/RES/2/370 for carrying out this work. Three of us (BM, NI and NA) are also highly thankful to IUCAA, Pune for providing the necessary facilities in completing this work.

**REFERENCES**

- Agrawal P. C., 2006, *AdSpR*, 38, 2989  
Cannizzo J. K., Wheeler J. C., 1984, *ApJS*, 55, 367  
Cunningham, C., 1976, *ApJ*, 208, 534  
Drappeau S., Malzac J., Belmont J., Gandhi P., Corbel S., 2014, *arXiv*, [arXiv:1412.5819](https://arxiv.org/abs/1412.5819)  
Dubus G., Lasota J. P., Hameury J.-M., Charles P., 1999, *MNRAS*, 303, 139  
Frank J., King A. R., Raine D., 2002, 3<sup>rd</sup> edition, P.60  
Gilfanov M., Arefiev V., 2005, *astro*, [arXiv:astro-ph/0501215](https://arxiv.org/abs/astro-ph/0501215) 9  
Hayakawa, S., 1981, *PASJ*, 33, 365  
Hoshi, R., Inoue, H., 1988, *PASJ*, 40, 421  
Hubeny, I.; Wickramasinghe, D. T., 2004, *RevMexAA*, 20, 200  
Ichikawa S., Osaki Y., 1994, *PASJ*, 46, 621  
Kanbach G., Straubmeier C., Spruit H. C., Belloni T., 2001, *Natur*, 414, 180  
Ko Y.-K., Kallman T. R., 1991, *ApJ*, 374, 721  
Lightman A. P., 1974, *ApJ*, 194, 419  
Low Mass X-Ray Binary Catalog, 4<sup>th</sup> edition, 2007  
Lyubarskii Y. E., 1997, *MNRAS*, 292, 67  
Mescheryakov A. V., Shakura N. I., Suleimanov V. F., 2011, *AstL*, 37, 311  
Mineshige S., Kusunose M., 1993, *PASJ*, 45, 113  
Motch C., Ilovaisky S. A., Chevalier C., 1982, *A&A*, 109, L1  
Ritter, H., 2008, [arxiv:08031970v2](https://arxiv.org/abs/08031970v2)[astro-ph]  
Shahbaz T., Charles P. A., King A. R., 1998, *MNRAS*, 301, 382  
Shakura N. I., Sunyaev R. A., 1973, *A&A*, 24, 337  
Soon-Wook Kim, Wheeler, J., C., Mineshige, S., 1999, *PASJ*, 51, 1  
Tuchman Y., Mineshige S., Wheeler J. C., 1990, *ApJ*, 359, 164  
Vrtilek S. D., Raymond J. C., Garcia M. R., Verbunt F., Hasinger G., Kurster M., 1990, *A&A*, 235, 162  
Wickramasinghe, D.; Hubeny, I., 2005, *ASPC*, 330, 219  
Zhang C. M., et al., 2011, *A&A*, 527, A83